Project	Lithium-ion battery's life cycle: safety risks and risk management at workplaces
Work package	WP2: Life cycle assessment
Task	T. 2.1 Determination of the material flows over the life cycle (also considering emissions, even in accidents)
Responsible organisation	GAIKER
Authors	Leire García, Leire Barruetabeña, Isabel Rodriguez Llopis

Abstract

The aim of this report is to evaluate the main flow of materials over the life cycle of Lithium-ion batteries (LIBs), and to identify the demand of key materials and the losses and potential points of recovery. The results will help identify the strategic materials in the supply chain that can lead to improvement strategies.

The results of the study are also related to the geographical definition of the supply chain carried out within D.1.1, as the locations of the points of extraction, consumption, release, and recovery of the strategic materials are also a key factor for identifying potential improvement strategies.

Finally, the data gathered within the Material Flow Assessment (MFA) will form the starting point of the Life Cycle Assessment (LCA) to be carried out in Task 2.2.

Table of contents

1 Methodology

The study aimed to evaluate the main material flows over the life cycle of lithium-ion batteries (LIBs). The evaluation was focused on a specific battery type and application, depending on the case study selected, which in this case was the NMC-811 battery to be used in off-road vehicles, as forklifts.

The Material Flow Assessment (MFA) is a widely used tool in circular economy studies that quantify material flows, and it includes the comprehensive measurement of input and output flows into a specified space and time framework, expressed as a physical unit (usually mass).

The MFA considers waste effluents and emissions to be part of the output side, and quantifies material consumption as input. The methodology offers transfer factors for the assessed material flows between the different processes within the scope of the study, which enables designing process inventories and ensures the preservation of the mass balance. In this context, the outcomes of the MFA were used as the basis for the LCA developed within this project (D.2.2).

In general, MFA methods can be divided into two types: the Substance Flow Assessment (SFA), which follows a single element or compound through the system; and the System-wide MFA, which accounts for all materials entering and leaving the system (Schmidt et al. 2021). This study was based on the System-wide MFA over the key life cycle stages of batteries, and did not consider 'unused extraction' (or displaced resources that do not enter the system as priced resources and goods).

The limits of the study, which was conducted as part of this project, were in the economic system, starting when materials entered the component production, and ending when materials emerged from the life cycle of the product. The fate of the output materials in the environment was not within the scope of the study.

2 Description of material flow over supply chain

2.1 Production phase

This section presents the main material flow over the life cycle of NMC-811 batteries. The flows were calculated as kg of intermediate product produced per supply chain step. The overall material flow for the average mass of a forklift battery (NMC-811) is presented later in Section 4.

Table 1 shows the basic characteristics of the reference battery considered in the study.

Table 1. Characteristics of studied LIB battery.

NMC-811	
Weight (kg)	684
Main constituents:	
Cell Materials (%)	**76.1**
Cathode (%)	44.7
Anode (%)	36.4
Electrolyte (%)	17.1
Separator (%)	1.8
Non-cell Materials (%)	**23.9**

The MFA requires a significant amount of information on consumptions and emissions over the life cycle, but due to the international distribution of the agents in the supply chain, and the high confidentiality of the requested information, it was not possible to gather primary data for the study. Thus, secondary data were gathered from the existing literature. Dai et al., (2019) and Accardo et al., (2021) were the most relevant data sources for this assessment.

Based on the literature, in order to estimate the material loss during the production of the components being integrated into the LIB, as well as the acceptance rate of the battery, average material yields are considered for each component (

Table 2).

Table 2. Average material yield in production processes.

NMC-811	
Main constituents:	**Yield (%)**
Active cathode material	92.2*
Active anode material	92.2**
Aluminium foil	90.2
Copper foil	90.2
Separator	98***
Electrolyte	94****
Acceptance rate	95*****

*Applies to active cathode material and NMP.
**Applies also to water.
***Applies to PP an PE.
****Applies to LiPF6, EC and DMC.
*****Applies to all the components in the battery's manufacturing phase

2.1.1 Production of cathode active material

The first step of the production of a cathode active material involves two main processes: 1) the production of the precursor by mixing the metal sulphates and the sodium hydroxide; 2) the production of NMC-811 by mixing the dried precursor with lithium hydroxide followed by calcination (see Figure 1).

A solid-state synthesis route was considered in this project. However, the main component of the active cathode material, LiNi1-x-yCoxMnyO2, can be synthesized using different methods, such as the hydroxide co-precipitation route, the oxalate co-precipitation route, and the solid-state method (Chuan-yue et al., (2011).

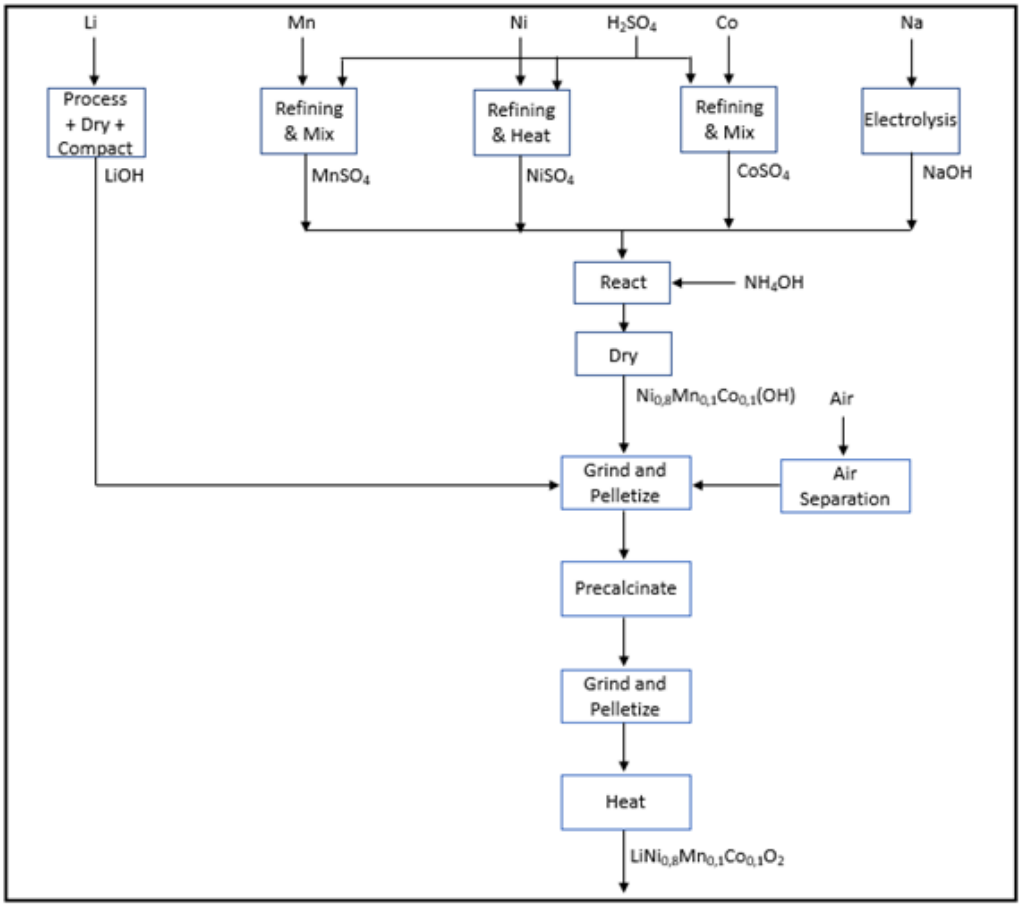

Figure 1. Production of NMC811 precursor using solid-state synthesis method. Modified from Dunn, et al., (2014).

The data input and output in this phase was mainly based on the information published by Dai et al., (2019) (Table 3).

Table 3. Mass components required to produce 1kg of cathode active material.

Component	Component Mass (kg)	Source
Inputs		
Lithium Hydroxide	0.246	Dai, et al., (2019)
Sodium Hydroxide	0.845	
Nickel Sulphate	1.273	
Cobalt Sulphate	0.159	
Manganese Sulphate	0.155	
Ammonium Hydroxide	0.117	
Process Water	0.757	

As the Ecoinvent 3.7 database does has no production process to obtain Cobalt Sulphate production was modelled from Zhang et al., (2021).

2.1.2 Production of the cathode

The cathode was composed of an aluminium current collector with a coat of positive electrode paste.

The synthesis process of the battery cathode, and more specifically, the NMC cathode, has evolved over the last years, and today several synthesis methods can be used: combustion, sol-gel, hydrothermal/solvothermal, and emulsion drying, the most common being co-precipitation, followed by spray pyrolysis and solid-state reaction methods. In recent years, the co-precipitation method has gained popularity for the synthesis of the NMC cathode, and is often used for batch production of cathode materials (Malik, et al., (2021)). Given the already mentioned significant data gaps, this study focused on the average material flow for this step, disregarding the process details.

The production of the cathode requires mixing a few components (binder and solvent, carbon black and graphite) in a ball mill into a slurry, followed by coating the collector foil (with aluminium forming its majority) with the slurry. The binder (modified styrene butadiene copolymer) is water soluble and has the advantage of needing no organic solvent.

Figure 2 shows the general scheme of the production process of the cathode.

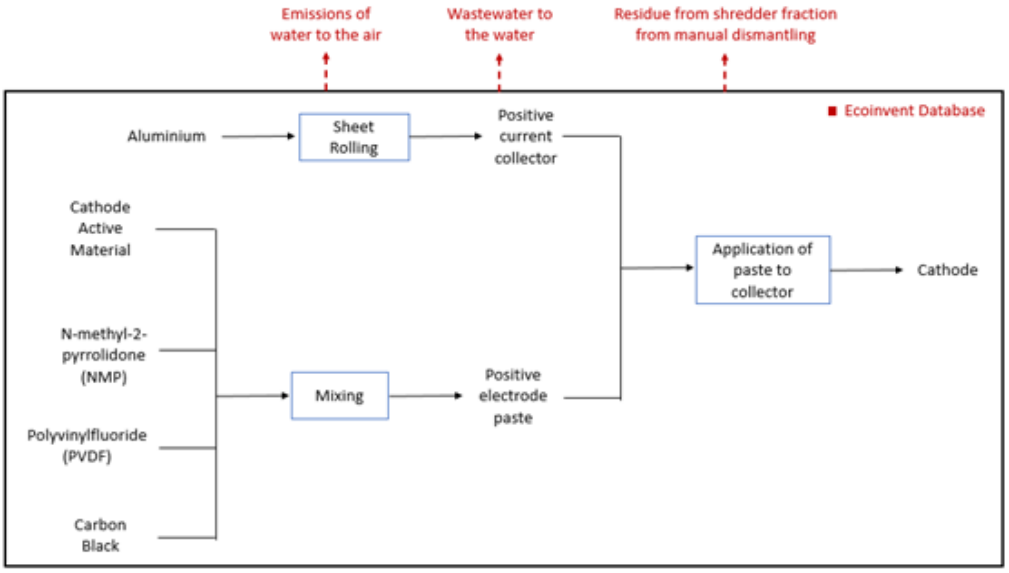

Figure 2. Cathode production process. Modified from Ellingsen, et al., (2013).

As Figure 2 shows, outputs other than the main product were also taken into account, based on Ecoinvent 3.7 data, in order to create a more complete cathode production process (see Table 4).

Table 4. Material input for producing 1kg of cathode. Source: Dai, et al., (2019) and Accardo, et al., (2021).

Component	Component Mass (kg)	Source
Cathode Active Material	0.7908	Based on Dai, et al., (2019)
Carbon Black	0.0432	
PVDF	0.0915	
Aluminium	0.2131	
NMP	0.0076	Based on Accardo, et al., (2021)

2.1.3 Production of the anode

Most LIBs rely on graphite negative electrodes to be used as anodes. Although natural graphite is the preferred anode material for LIBs, due to its significantly lower price, a considerable amount of synthetic graphite is also used. Its market share is expected to

grow in the future, due to its better electrochemical performance and resource security concerns.

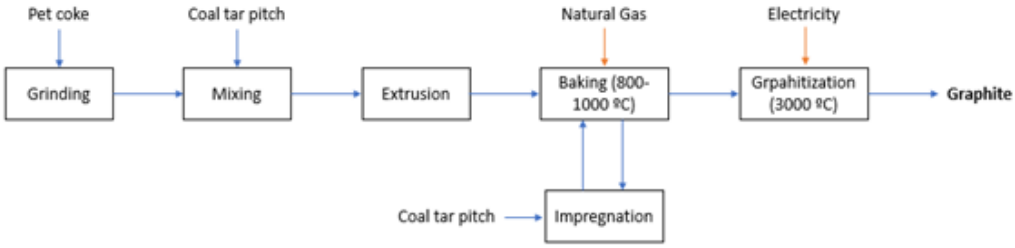

Figure 3. Block diagram of graphite production. Modified from Dunn et al., (2014).

As shown in Figure 3, the process starts by grinding the pet coke, which is later sent to the mixer to be blended with the coal tar pitch in the desired proportions. The mixers are heated to keep the mixture in a liquid state, allowing the pitch to penetrate the pores of the coke during mixing. Before feeding the mixture into the extruder, it is cooled from 160–170 ºC to around 100 ºC. The cooled mixture is then fed into the extruder, and subsequently heated to 800–1000 ºC in a natural gas-fired furnace. During this baking, the coal tar pitch is converted into coke, and loses 30–40% of its weight. Furthermore, to improve the properties of the final graphite, the baked mixture is often impregnated with pitch and rebaked before it is sent to the graphitization furnace. In this furnace, the mixture is fired to around 3000 ºC and forms graphite crystals, which are the final product of the process (Dunn, et al., (2014)).

Once the graphite has been produced, it is mixed with the solvent and the collector, as shown in Figure 4.

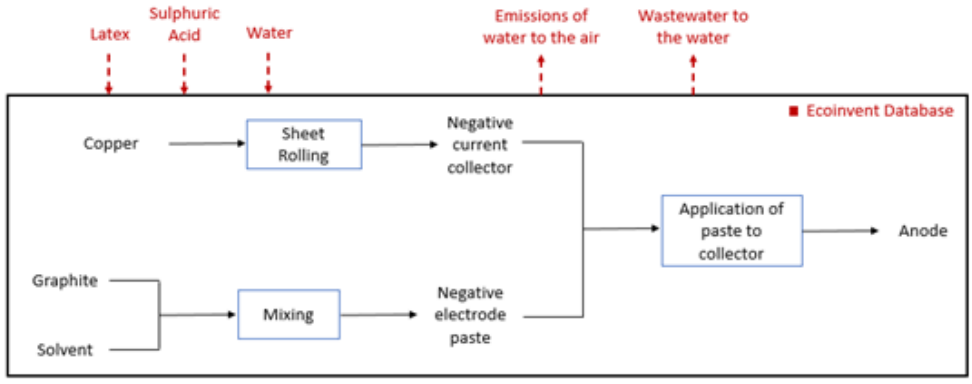

Figure 4. Anode production process. Modified from Ellingsen, et al., (2013).

The main inputs in the process were calculated using the same methodology as that used in the previous processes (see Table 5), and further inputs related to the consumption of auxiliary material and emissions were also incorporated, on the basis of the Ecoinvent 3.7 Database.

Table 5. Material input for producing 1kg of anode. Source: Dai, et al., (2019) and Accardo, et al., (2021).

Component	Component Mass (kg)	Source
Graphite	0.6426	Based on Dai, et al., (2019)
Copper	0.5006	
Water	0.0094	Based on Accardo, et al., (2021)

2.1.4 Production of the electrolyte

Electrolytes are composed of salt, solvents, and additives, as shown in Figure 5.

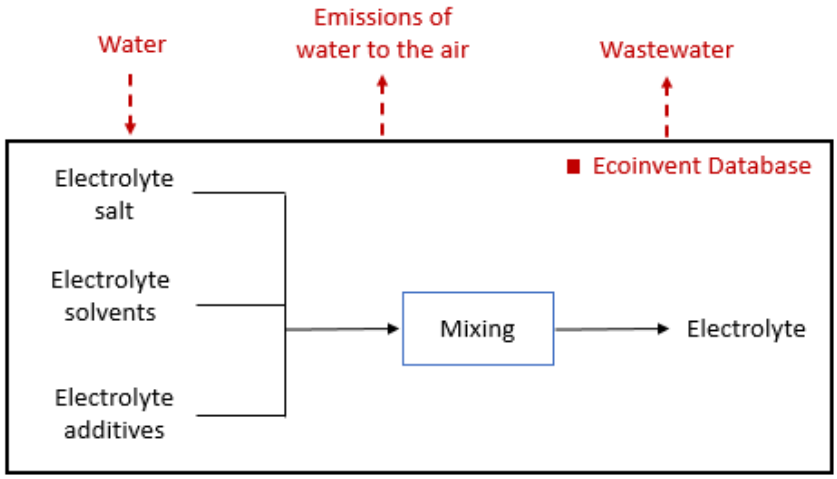

Figure 5. Electrolyte production process. Modified from Ellingsen, et al., 2013.

At present, electrolyte commercial salt is usually based on $LiPF_6$. Electrolyte salt can be produced by different processes, but the principal one is based on PF_5 and LiF. In practical productions, PF_5 is usually obtained from PCl_5, due to its availability and low price, and HF is used as the fluorinating agent of PCl_5 (Liu, et al., (2019)). Once the $LiPF_6$ salt has been produced, it is mixed with the solvents and additives to form the electrolyte, as shown in Table 6.

As in the previous processes, the auxiliary inputs and outputs from the Ecoinvent 3.7 database were considered in this process.

Table 6 Material input for producing 1kg of electrolyte. Source: Dai, et al., (2019) and Crenna, et al., (2021).

Component	Component Mass (kg)	Source
Lithium hexafluorophosphate	0.1713	Based on Dai, et al., (2019)
Ethylene carbonate (solvent)	0.4643	
Dimethyl carbonate (solvent)	0.4643	
Vinyl carbonate (additive)	0.02	Based on Crenna, et al., (2021)

2.1.5 Production of the separator

Separators are porous membranes that keep the active electrode materials apart to prevent short circuits and the potential associated thermal runaway. They are composed by polymers, and as assumed by Ellingsen (2013), they can be produced by injection moulding (see Figure 6). The main components of a separator are Polypropylene and Polyethylene. Both polymers are thermoplastics with high resistance to temperature, and therefore, do not fluster at high temperatures.

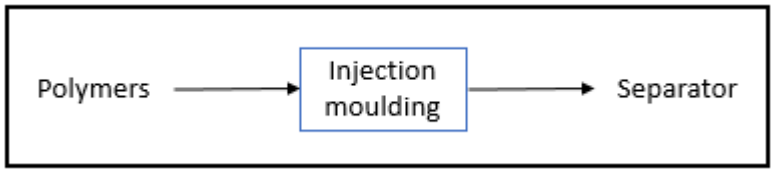

Figure 6. Separator's production process. Modified from Ellingsen et al., (2013).

As before, bibliographical data was used to calculate the masses needed to complete the production process. Table 7 presents these results.

Table 7 Material input for producing 1kg of separator. Source: Dai et al., (2019).

Component	Component Mass (kg)	Source
Polypropylene	0.8951	Based on Dai, et al., (2019)
Polyethylene	0.1790	

2.1.6 Production of the cell

The components obtained in the previous steps are used to produce the cell. The material flow to produce 1 kg of LIB cell was estimated on the basis of the literature data (Dai, et al., 2019), and is summarized Table 8.

Table 8 Material input for producing 1kg of cell. Source: Dai, et al., (2019).

Component	Component Mass (kg)	Source
Anode	0.364	Based on Dai, et al., (2019)
Cathode	0.447	
Electrolyte	0.171	
Separator	0.018	

2.2 Production of non-cell materials

Finally, once the cell has been composed, the non-cell materials have to be added to assemble the battery pack. Table 9 shows the materials needed as non-cell elements to complete the battery, according to the literature source (Accardo et al., 2021).

Table 9 Material input for producing 1kg of non-cell materials. Source: Accardo et al., (2021).

Component	Component Mass (kg)	Source
Inputs		
Copper	0.0126	Accardo, et al., (2021)
Aluminium	0.7824	
Steel	0.0251	
PET	0.0209	
Electronics	0.1590	

2.3 Use phase

The use phase presents few opportunities for material input and output, other than accidents or repair. No data on battery repair were available, and at this stage, no repair was considered. In this context, it was assumed that damaged batteries were disposed of and treated. However, a risk of accidental leakage, explosion and/or fire has already been reported by different sources. In fact, the stable structure of LIBs can be damaged by different factors (physical, electrical, and thermal), generating a thermal hazard, which in most cases leads to the emission of different toxic gases.

Temperature is the key factor in many accidents. Increased temperature causes a short circuit, which may lead to an even higher temperature and pressure, ending in a potentially flammable gas release. Damage in the separator, leakages, etc. can also lead to similar incidences.

The toxicity of the emitted gases varies, being related to the emission of gases from HF to water vapor. In order to obtain quantitative data for the material flow during the use phase, different literature sources were reviewed, for example, Essl, et al., (2020), Sun, et al. (2016) and Amano et al. (2022). The outcomes of these studies formed the basis for calculating the gas releases during accidents leading to explosion or ignition.

However, the accident rate leading to material release (mainly explosion or ignition) is also a key factor to be considered. The case study selected for this project was an electrified forklift with an NMC-811 battery, but no statistical information on the accident rates of this kind of vehicle was available. In this context, the extrapolation of the accident rate of electric vehicles (EVs) was proposed as an approximation to fill this data gap and was based on the expected durability and average daily use of both types of vehicle.

A life span of 10,000 hours for electric forklifts was used as a starting point (Sullivan, 2016), although this value may vary depending on the producer and the specifications of the vehicles. On the other hand, some producers guarantee durability for their electric vehicles of eight years or 100.000 miles, such as Nissan and Tesla (EDF, 2022). Considering that a car is used for two hours/day, the lifespan of an EV would be approximately 5840 hours.

On the other hand, three electric car fires occur per 1000 starts (AutoinsuranceEZ, 2022), i.e., an 0.03% chance of ignition (CNBC, 2022). Based on these estimations, the probability of explosion/ignition is considered 0.051% over the lifetime of a forklift.

This explosion/ignition probability was the starting point for building the use phase scenario, in order to later apply the accident-related gas release rate mentioned in this chapter.

Table 7 summarizes the values obtained.

Table 10. Calculated values of gases released during forklift's use phase.

Component	Min Component Mass (g)	Max Component Mass (g)	Average Component Mass (g)
CO	9.0011	58.3559	33.6785
CH_4	1.2205	5.2736	3.2470
H_2O	3.2380	4.3435	3.7909
HF	0.0290	0.1880	0.1085
HCN	0.0117	0.0762	0.0439
C_2H_6	0.5190	1.0326	0.7758
C_2H_4	1.3891	21.1994	11.2942
H_2	0.5150	3.3388	1.9269
CO_2	12.7556	82.6977	47.7267
EMC	0.9098	5.8982	3.4039
C_4H_{10}	0.3564	2.3107	1.3335
		SUM	**107.33**

2.4 End of life

Recycling LIBs is a complex and costly process. The wide range of LIB composition and designs (combined with the already mentioned lack of information on these aspects), creates additional difficulties for determining efficient material recovery processes (Lebedeva et al., 2017)(see *Table 11*).

Although the volume of spent LIBs is still low, it is expected to rise dramatically in coming years (see Section **Error! Reference source not found.** for further details), together with the demand and value of the strategic materials that LIBs contain. For this reason, optimizing material recovery will become a key issue.

Today, different recycling technologies are implemented internationally. Most existing hydrometallurgical processes prioritize Co recovery through leaching and precipitation, while Li tends to remain in the leaching solution together with the impurities. However, in the pyrometallurgy processes, the main focus is on Co and Ni recovery, while Li is lost in the slag (Nasser & Petranikova, 2021). Furthermore, some companies have developed combined technologies that include both processes (e.g., Umicore). For this case study, the Umicore process was considered, mainly due to its data availability and relevance in Europe.

Table 11. Efficiency of recycling for various elements in NMC and LFP batteries (Lebedeva, et al., (2017)).

Material	Combination of pyrometallurgical & hydrometallurgical processes – NMC and LFP [%]	Purely hydrometallurgical process – NMC only [%]	Purely hydrometallurgical process – LFP only [%]
Lithium	57	94	81
Nickel	95	97	NA
Manganese	0	~ 100	NA
Cobalt	94	~ 100	NA
Iron	0	NA	0
Phosphate	0	NA	0
Natural graphite	0	0	0

Umicore NV is a multinational material processing group. In 2011, a battery recycling pilot plant was tested in Hofers, Sweden and later upscaled and installed in Hoboken, Belgium. Although the Hoboken plant has announced a permitted capacity of 7000 ton/year for LIBs, the current treatment capacity is unknown (Sojka et al., 2020).

Umicore's pyrometallurgical-hydrometallurgical process can take both LIBs and nickel hydride batteries. The pyrometallurgical part of this process produces a nickel-cobalt-copper-iron alloy, and subsequent hydrometallurgical processes further refine these metals (Pinegar & Smith, 2019). In addition to the batteries, additives such as coke, sand, and limestone are fed into the smelting furnace (Sojka et al., 2020).

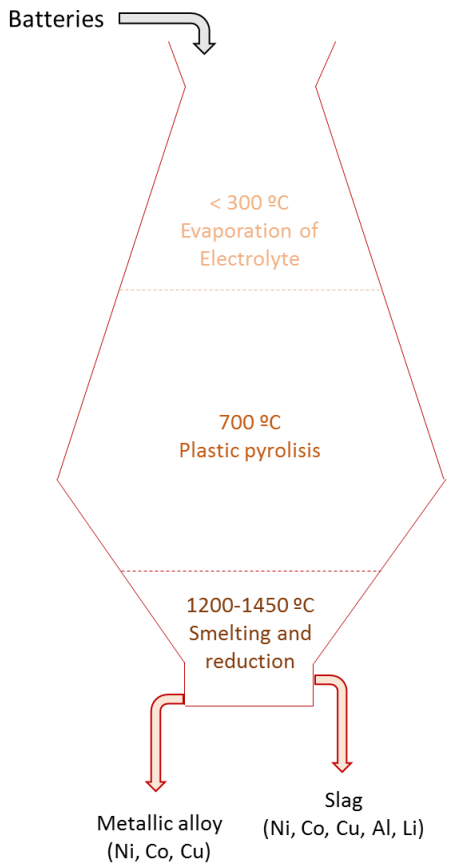

Figure 7. Schematic diagram of Umicore's shaft furnace. Modified from Sojka et al. (2020).

The smelter can be divided into three zones (see Figure 7): 1) the upper zone (<300 ºC), where the electrolytes are evaporated; 2) the middle zone (700 ºC), where the plastics are pyrolyzed; and 3) the bottom zone (1200–1450 ºC), where smelting and reduction take place.

In this case, the organics (electrolyte solvents and plastic housings) and graphite are used as combustible compounds and reducing agents for metal oxides. According to the literature, the energy released during these reduction reactions provides sufficient energy to heat the smelter (Sojka et al., 2020).

The process has a gas cleaning system in order to fully decompose the organic compounds and ensure that no harmful dioxins or volatile organic compounds are produced. The output flows or fractions that the smelter generates can be summarized as follows (Sojka et al., 2020):

- **Metallic alloy:** containing Co, Ni and Cu, can be forwarded to the downstream hydro-metallurgical process for the recovery of Co, Ni as principal materials, and also Cu.
- **Slag:** containing Al, Li, Mn, is generally disposed of or sold as construction material (Sojka et al., 2020). It can be processed further for metal recovery, but as this is a cost- and energy-intensive alternative, it is not usually done (Pinegar & Smith, 2019).
- **Cleaned gas:** off-gas is cleaned using UHT technology. The flue dust resulting from the cleaning system, which contains the halogens (mainly Fluorine), is landfilled.

The metallic alloy is treated by an acid leaching processes to remove copper, iron, zinc, and manganese prior to the solvent extraction process. This solvent extraction process with sulphuric acid separates nickel from cobalt with a high purity. Figure 8 shows a schematic diagram of the overall process (Pinegar & Smith, 2019):

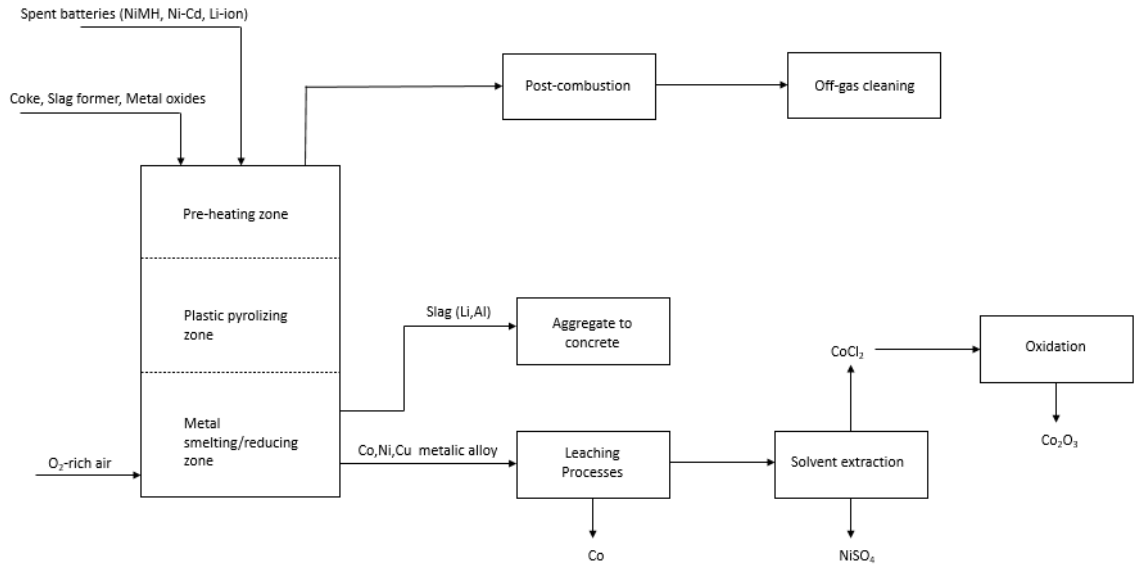

Figure 8. Block diagram of Umicore's recycling process. Modified from (Pinegar & Smith, 2019).

The main drawbacks of this process are that its economic feasibility is strongly driven by the prices of cobalt and nickel, and it does not recover other valuable metals such as lithium (Pinegar & Smith, 2019). However, the LIB volume for treatment and the economic value of the different strategic materials it contains are expected to change in coming years, leading to a different scenario.

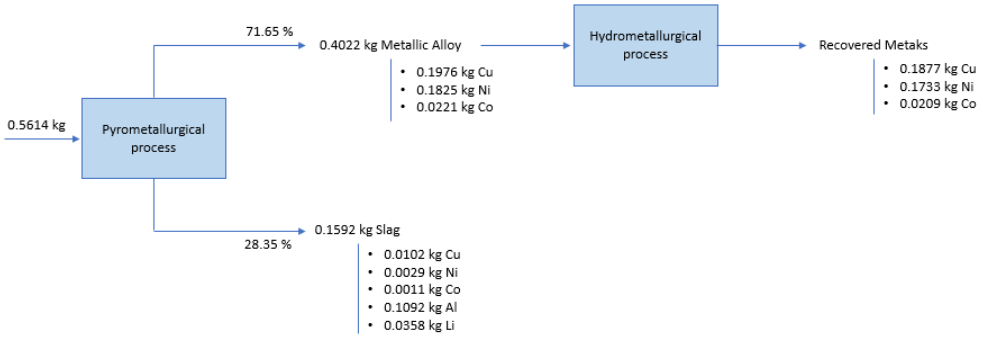

Figure 9. Mass flow diagram of recycling process.

The mass flow was modelled using bibliographical data and data from Umicore's Patents (Daniel Cheret & Sven Santen, 2007). Figure 9 shows the material flow per kg of LIB processed: Mass flow diagram of the recycling process.

The outputs from the treatment of the LIB assessed in this study were calculated on the basis of the transfer coefficients of the pyrometallurgical process extracted from the Umicore patent (Daniel Cheret & Sven Santen, 2007):

- Metallic Alloy:
    - 95.1% Cu = 102.85 kg
    - 98.43% Ni = 94.97 kg
    - 95.37% Co = 11.49 kg

      TOTAL = 209.31 kg (71.65% of total entrance)
- Slag:
    - 4.9% Cu = 5.3 kg
    - 1.57% Ni = 1.51 kg
    - 4.63% Co = 0.56 kg
    - 100% Al = 56.802 kg
    - 100% Li2O = 18.644 kg

      TOTAL = 82.82 kg (28.35% of total entrance)

These values enable the characterization of the main outputs from the pyrometallurgical process, namely the metallic alloy (49.14% Cu, 45.37% Ni, 5.49% Co) and the slag (6.4% Cu, 1.83% Ni, 0.67% Co, 68.59% Al, 22.51% Li2O)

The final results of the hydrometallurgical process, considering that it will have a 95% degree of accuracy, are shown in Figure 9. Note that the data in the image are for 1 kg of battery.

As preparation was limited due to the large size of industrial batteries, cell-level dismantling was assumed.

3 Overall material flow of NM-811 LIB over life cycle

Determination of the material flows over the life cycle

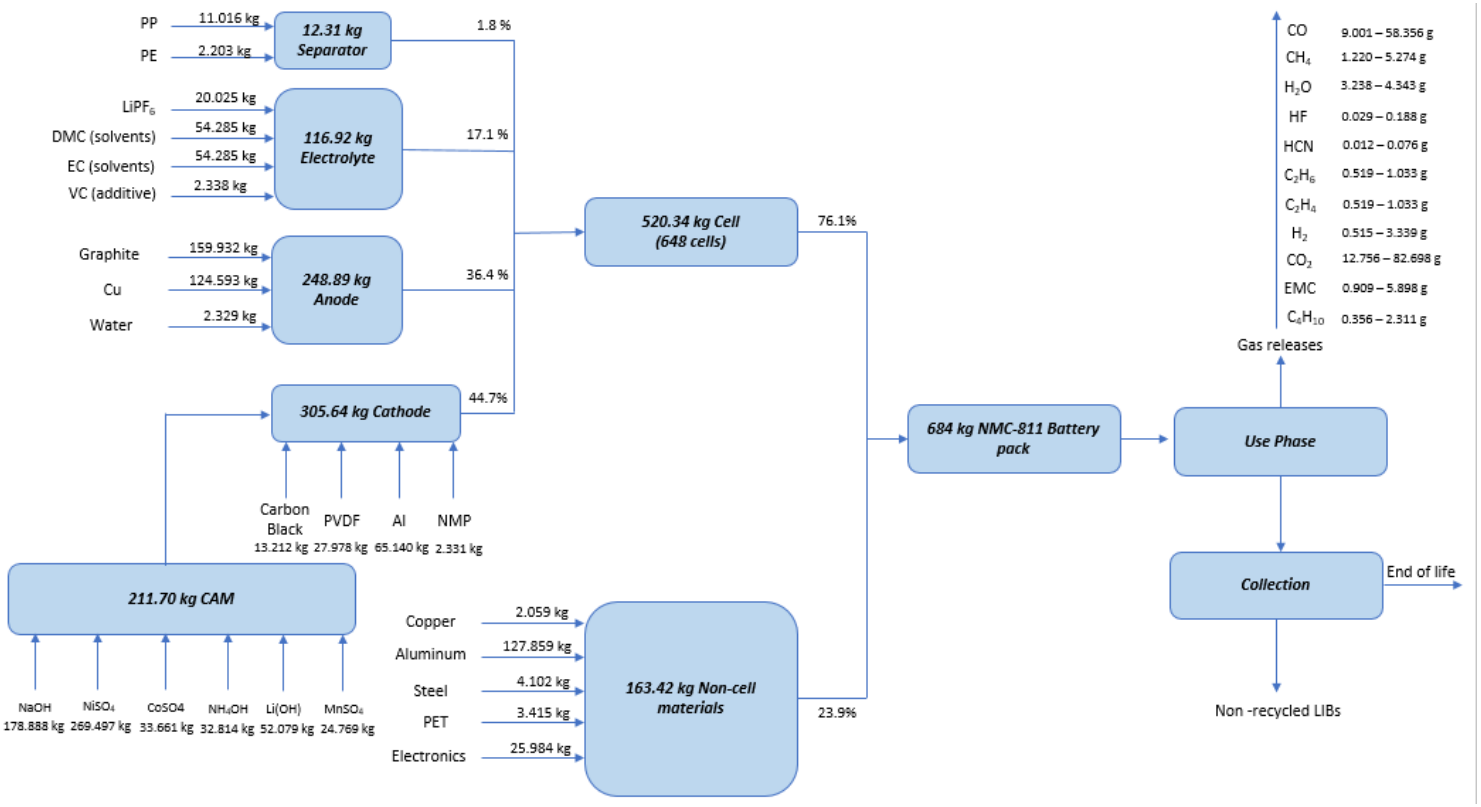

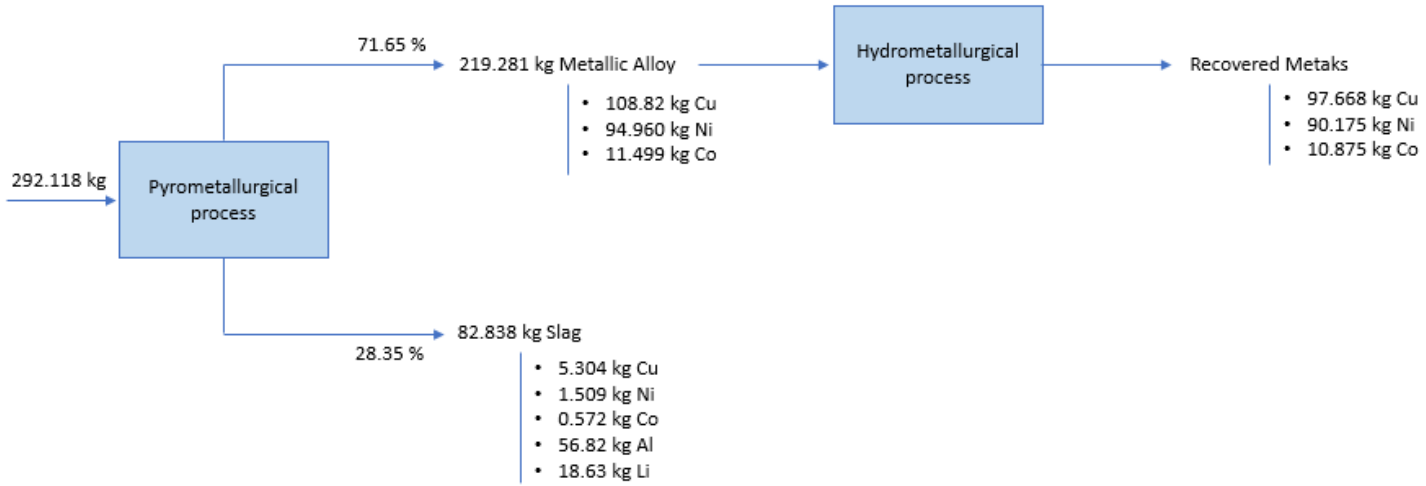

Figure 10. General mass flow diagram of process

4 Future inquiries about main components

The production of LIBs is leading to an increased demand of critical metals all over the world, as shown in the figures below (Figure 11).

Future demand forecast:

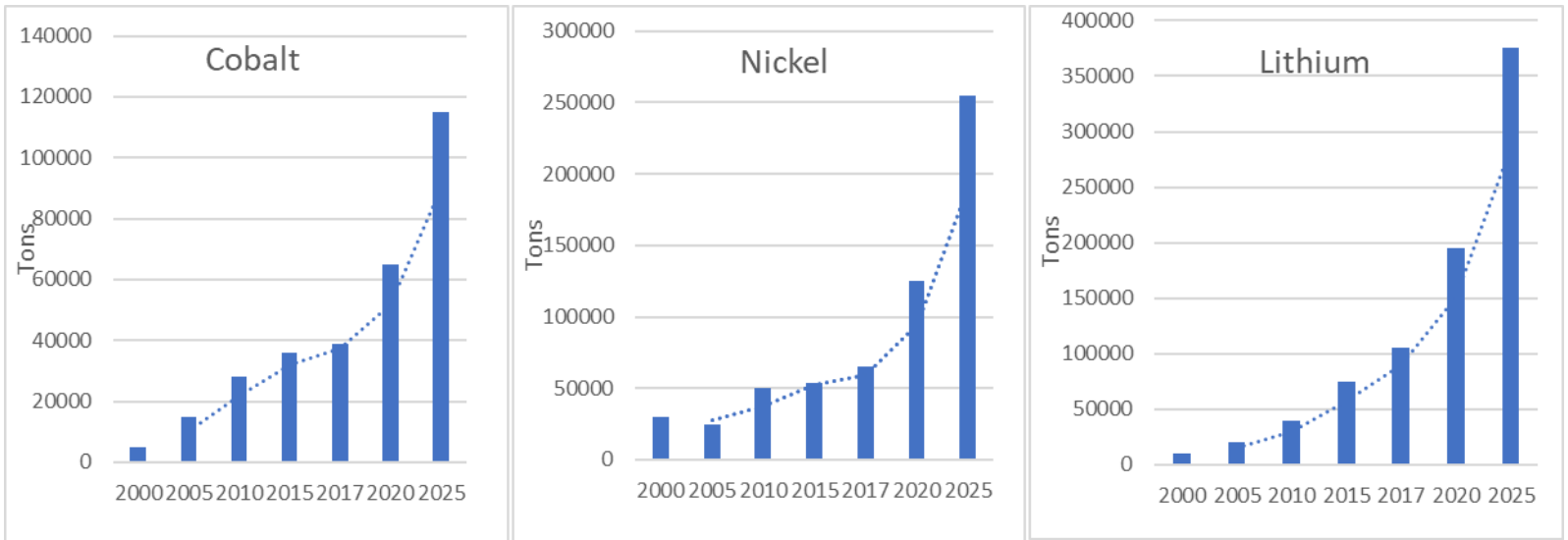

Figure 11. Current and prospective demand of some strategic materials. Modified from (European Commission, 2018).

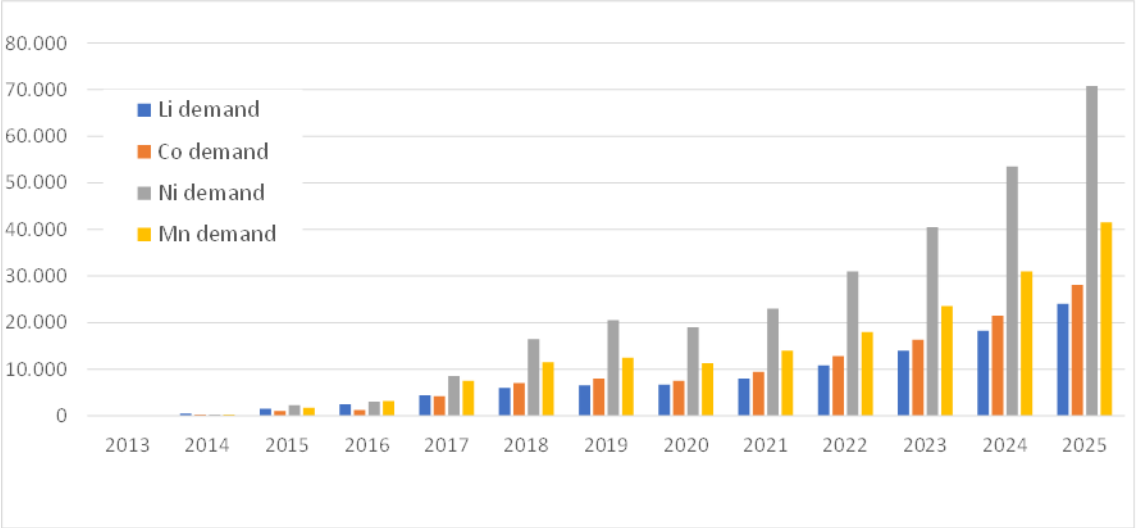

Figure 12. Current prospective metal demand in China's new energy automobile industry (historical data 2013–2025, prospective data 2021–2025). Modified from (Hu, et al., 2021).

Most of these metals are obtained from non-European countries. Lithium resources, for example, are mainly concentrated in South America, as a great proportion of its reserves are concentrated in Chile (European Commission, 2018).

This augmented demand is also linked to rising prices, and in this context, the European dependency on external sources constrains the development foreseen in the mobility sector.

The exploitation of Li resources in Europe is expected to increase in coming years, although the global reserves in the EU are rather limited (European Commission, 2018). It should be taken into account that disposed LIBs could also offer a valuable source of material if suitable and efficient recycling processes were available. However, today many critical metals are not being recovered at the end of life of LIBs. For example, the MFA of the recycling process considered in this study shows that an important loss of resources is associated with the metals that form the slag, namely lithium, aluminium and manganese.

Although the demand for and the price of lithium (and other key metals for LIBs) have drastically increased in recent years (**Error! Reference source not found.** and **Error! Reference source not found.**), the efficiency of the material recovery in the end of life processes has not shown the same trend.

However, in the medium term, the significant amount of Li and other critical materials that will be consumed in coming years will arrive at recycling installations, leading to a waste fraction with a high concentration of strategic metals. At this point, it is expected that the focus will clearly be on maximizing the recovery of these metals, given the economic value that they will have achieved at that point.

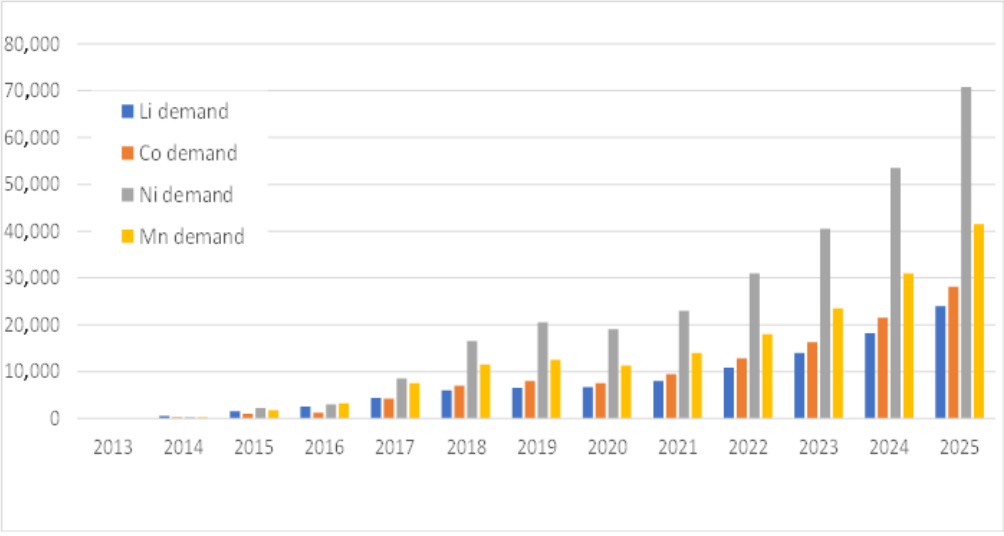

Figure 13. Lithium price evolution since 2021. Modified from (Daily Metal Prices, 2022).

The consumption of metals for the elaboration of batteries is also increasing (**Error! Reference source not found.** and **Error! Reference source not found.**), and if this does not change, the prices of all metals will increase in the same way or drastically more. In the next years, the consumption and demand of these metals is expected to increase even more and the way of retrieving them will need to evolve, but this is not predicted to happen.

5 Conclusions

The MFA of the selected NMC-811 LIB shows that the increasing trend towards electrifying vehicles' fleets requires considering the material inputs and outputs throughout the value chain in order to ensure the sustainability of this transition.

A significant number of materials is required to produce this type of battery, but confidentiality makes data gathering complex, both in the production and end-of-life phases. The inventory of the MFA in this study was based on bibliographical sources, and the actual demand (and loss) of materials may be even higher than that reported. In this context, enabling the recovery of different losses over the value chain through recycling strategies is essential, as is maximizing their efficiency, especially at the battery's end of life.

Although recycling Li and other strategic materials does not currently seem to be of great interest to companies (due to low concentration in waste flow, lack of efficient processes, etc.), this situation is expected to change in the future, as the amounts of battery waste increase and the demand of strategic metals rises. For this reason, and to prepare for this future scenario, it is crucial that the efficiency of the recycling process be improved.

As stated above, data limitation constrains accurate MFA over the life cycle, and in this context, greater involvement of different actors along the supply chain would be necessary for data transparency. In the future, initiatives such as the Battery Passport may contribute to solving this problem.

For the use phase, extensive research has been carried out on the potential risks associated with the use of LIBs (leachate, explosion, fire, gas emission, etc.). However, in this case, there was no reliable or quantitative information on the real incidence of these risks and the mass loss (liquid, solid or gas) that may occur. The estimation made in the project reflects a low mass flow in these steps, although each impact on human health and the environment can be of great importance. This last aspect, however, will be further evaluated in the LCA carried out as part of this project.

Table 12 and Table 13 summarize the material losses of the strategic materials in the LIB value chain.

Table *12* shows the relative loss of each material in each step of the value chain (ratio of material loss/input in each step). Table 13 in turn shows the general overview of the material loss over the value chain (material loss in each step/total input in the value chain).

Table 12. Summary of main losses in production of selected LIB.

LOSSES (%)	PRODUCTION				USE PHASE	END OF LIFE
	CAM production	Cathode production	Anode production	Electrolyte production		
Li	64.2	29.7	-	28.3	0.05	100
Co	64.2	29.7	-	-	0.05	9.8
Cu	-	-	31.2	-	0.05	9.7
Ni	64.2	29.7	-	-	0.05	6.5
Al	-	31.2	-	-	0.05	100
Mn	64.2	29.7	-	-	0.05	100

Table 13. Summary of global losses throughout value chain of selected LIB.

LOSSES (%)	TOTAL		
	PRODUCTION	USE PHASE	END OF LIFE
Li	49.3	0.05	50.65
Co	64.2	0.05	3.45
Cu	13	0.05	8.55
Ni	64.2	0.05	2.25
Al	4.3	0.05	95.65
Mn	64.2	0.05	35.75

The main losses in production are in CAM production. In fact, these losses duplicate the losses in cathode production. Further information would be necessary to evaluate the material recycling within this step to get a more accurate idea of the relevance of these losses.

On the other hand, the loss rates at the end-of-life phase are significant. This is due to the inefficiency of the recycling process in recovering some critical materials such as Li, Al, and Mn. Only Ni and Li show a significant recovery rate at end of life.

Bibliography

Accardo, A., Dotelli, G., Luigi Musa, M., & Spessa, E. (2021). Life Cycle Assessment of an NMC Battery for Application to Electric Light-Duty Commercial Vehicles and Comparison with a Sodium-Nickel-Chloride Battery. *Applied Sciences, 11*, 1160.

Amano, K. O., Hahn, S.-K., Tschirschwitz, R., Rappsilber, T., & Krause, U. (2022). An Experimental Investigation of Thermal Runaway and Gas Release of NMC Lithium-Ion Pouch Batteries Depending on the State of Charge Level. *Batteries, 8*, 41.

AutoinsuranceEZ. (2022). *Gas vs Electric Car Fires* . Retrieved from AutoinsuranceEZ.com: https://www.autoinsuranceez.com/gas-vs-electric-car-fires/

Chuan-yue, H., Jun, G., Yong, D., Hong-hui, X., & Yue-hui, H. (2011). Effects of synthesis conditions on layered Li[Ni1/3Co1/3Mn1/3]O2 positive-electrode via hydroxide co-precipitation method for lithium-ion batteries. *Elseiver, 21*, 114-120.

CNBC. (2022). *Electric vehicle fires a rare, but hard to fight - here's why*. Retrieved from Why electric vehicle fires are so challenging: https://www.cnbc.com/2022/01/29/electric-vehicle-fires-are-rare-but-hard-to-fight-heres-why.html

Crenna, E., Gauch, M., Widmer, R., Wäger, P., & Hischier, R. (2021). Towards more flexibility and transparency in life cycle inventories for Lithium-ion batteries. *Elseiver, 170*, 105619.

Dai, Q., Spangenberger, J., Ahmed, S., Gaines, L., C. Kelly, J., & Wang, M. (2019). *EverBatt: A Closed-loop Battery Recycling Cost and Environmental Impacts Model*. Argonne: Argonne National Laboratory.

Daily Metal Prices. (2022). Retrieved from amaramar.com/webcam-playas/euskadi/bizkaia/atxabiribil

Daniel Cheret, S., & Sven Santen, H. (2007). *United States of America Patent No. 7,169, 206*.

Dunn, J. B., Gaines, L., Barnes, M., Sullivan, J., & Wang, M. (2014). *Material and energy flows in the materials production, assembly and end of life stages of the automotive lithium-ion battery life cycle*. Argonne: Argonne National Laboratory.

EDF. (n.d.). *EDF, All about electric car batteries*. Retrieved from https://www.edfenergy.com/electric-cars/batteries#:~:text=The

Ellingsen, L. A.-W., Majeau-Bettez, G., Singh, B., Srivastava, A. K., Valøen, L. O., & Strømman, A. H. (2013). Life Cycle Assessment of a Lithium-Ion Battery Vehicle Pack. *Journal of Industrial Ecology, 18*, 113-124.

Essl, C., Golubkov, A. W., Thaler, A., & Fuchs, A. (2020). Comparing Different Thermal Runway Triggers for Automotive Lithium-Ion Batteries. *ECS Transactions, 97*, 167-183.

European Commission. (2018). *Report on Raw Materials for Battery Applications.* Brussels.

Hu, S., He, S., Jiang, X., Wu, M., Wang, P., & Li, L. (2021). Forecast and Suggestions on The Demand of Lithium, Cobalt, Nickel and Manganese Resources in China's New Energy Automobile Industry. *IOP Conference Series: Earth and Environmental Science*.

Lebedeva, N., Di Persio, F., & Boon-Brett, L. (2017). *Lithium ion battery value chain and related opportunities for Europe.* Luxembourg: Publications Office of the European Union.

Liu, J., Cai, Y., Xiao, C., Zhang, H., Lv, F., Luo, C., . . . Yu, L. (2019). Synthesis of LiPF6 Using CaF2 as the Fluorinating Agent Directly: An Advanced Industrial Production Process Fully Harmonious to the Environments. *Industrial & Engineering Chemistry Research, 58*, 20491-20494.

Malik, M., Chan, K.H., Azimi, G. (2021). Effect of Synthesis Method on the Electrochemical Performance of $LiNixMn_yCo_{1-x-y}O_2$ (NMC) Cathode for Li-Ion Batteries: A Review. *Rare Metal Technology 2021* (pp. 37-46). Cham: Springer.

Nasser, O. A., & Petranikova, M. (2021). Review of Achieved Purities after Li-ion Batteries Hydrometallurgical Treatment and Impurities Effects on the Cathode Performance. *Batteries, 7*, 60.

Pinegar, H., & Smith, Y. R. (2019). Recycling of End-of-Life Lithium Ion Batteries, Part I: Commercial Processes. *Journal of Sustainable Metallurgy, 5*, 402–416.

Schmidt Rivera, X. C., Balcombe, P., & Niero, M. (2021). Chapter 3. Life Cycle Assessment as a Metric for Circular Economy. 10.1039/9781788016209-00054

Sojka, R., Pan, Q., & Billmann, L. (2020). *Comparative study of Li-ion battery recycling processes.* Germany: ACCUREC Recycling GmbH.

Sullivan, J. (2016, 12 13). *TOYOTA, How Long Will an Average Forklift Last?* Retrieved from https://www.tmhnc.com/blog/how-long-will-a-forklift-last-and-forklift-average-use

Sun, J., Li, J., Zhou, T., Yang, K., Wei, S., Tang, N., . . . Chen, L. (2016). Toxicity, a serious concern of thermal runaway from commercial Li-ion battery. *Elsevier, 27*, 313–319.

Zhang, T., Bai, Y., Shen, X., Zhai, Y., Ji, C., Ma, X., & Hong, J. (2021). Cradle-to-gate life cycle assessment of cobalt sulfate production derived from a nickel–copper–cobalt mine in China. *Springer*, 26, 1198–1210.